

Research Article

Radar Emitter Individual Identification Based on Convolutional Neural Network Learning

Wei Sun ¹, Lihua Wang ², and Songlin Sun ³

¹Yantai Vocational College, Yantai, Shandong, China

²China Unicom Digital Technology Co., Ltd., Beijing, China

³Beijing University of Posts and Telecommunications, Beijing, China

Correspondence should be addressed to Wei Sun; 15601001217@163.com

Received 1 July 2020; Revised 19 January 2021; Accepted 31 January 2021; Published 10 February 2021

Academic Editor: Paolo Crippa

Copyright © 2021 Wei Sun et al. This is an open access article distributed under the Creative Commons Attribution License, which permits unrestricted use, distribution, and reproduction in any medium, provided the original work is properly cited.

Radar Emitter Individual Identification is a key technology in modern electronic radar systems. This paper will focus on Radar Emitter Individual Identification (REII). Based on the advantages of Empirical Mode Decomposition (EMD) and bispectrum in signal processing, we propose an REII method based on the CNN. Firstly, the radar emitter signal is preprocessed. Secondly, the Hilbert–Huang Transform (HHT) spectrum and bispectrum are combined to form an image of the signal. Finally, in order to avoid loss of information and achieve the potential identification performance improvement, the signal image obtained is identified by the optimized CNN. Experimental results based on the measured signals show that the proposed method has high identification accuracy and is capable of meeting real-time identification requirements. The deep-learning-based identification method proposed in this paper has strong generalization ability and adaptability, which provides a new way for REII.

1. Introduction

In recent years, the fifth-generation mobile communication system (5G) has become a hot topic for discussion in the communications industry and academia. System interference in ultradense networks will severely reduce spectrum efficiency [1]. Spectrum sharing and unlicensed wireless networks associate technologies to address the smart spectrum sharing for 5G and affordable networks [2]. 5G has increased the development of high-frequency technology to solve the problem of insufficient supply of low-frequency to a certain extent. On the other hand, 5G relies on many base stations and lays enough antennas to make the network coverage area widely covered, allowing dense networks to work together, enhancing the strength of information signals, and ensuring the reliability of the information transmission process [3].

High-density networking and the use of high-frequency technology have led to an increasingly complex electromagnetic environment. With the upgrading of intelligence and automation of electronic reconnaissance technology, a

radar emitter signal waveform turns to be changing rapidly with massive parameters, and features are more concealed, which brings new difficulties and challenges to REII [4].

In order to achieve good identification performance, it is necessary to extract fingerprint features that can effectively reflect the subtle differences of tremendous devices [5]. This kind of differences is usually caused by unintentional modulation. The time-frequency analysis method has important applications in signal processing, including Short-Time Fourier Transform (STFT) [6, 7], Wigner–Ville Distribution (WVD) [8], S Transform (ST) [9], Continuous Wavelet Transform (CWT) [10], EMD [11], and so on. Hayaparan et al. [12] pointed out that the time-frequency characteristics of signals can be uniquely identified. Extracting signal fingerprint features from time-frequency distributions is a current research hotspot [13]. Therefore, this paper uses the extracted unique fingerprint features for identification. EMD has strong adaptability, and the obtained time-frequency map has a high resolution, which is suitable for processing nonstationary signals such as radar emitter signals. Therefore, this paper uses EMD to process

nonstationary signals such as radar transmitters. Bispectrum can retain phase information, suppress Gaussian noise, and is widely used in signal fingerprint feature extraction [14, 15]. Therefore, this paper uses the bispectral information of the signal as the fingerprint feature for signal unique identification. Generally, the computational complexity of bispectrum is high, so the integral bispectrum method is often used for dimensionality reduction, including RIB [16], AIB [17], CIB [18], and SIB [19]. Besides, the bispectral slice features can also be utilized as fingerprint features [20, 21]. Zhang et al. [22] investigate the specific emitter identification (SEI) problem, and three algorithms based on the Hilbert spectrum are proposed. Current identification methods often require manual design features, and feature engineering is complex and uncertain, resulting in poor generalization ability and adaptability. An improved quantum evolutionary algorithm (QEA) based on the niche coevolution strategy and enhanced particle swarm optimization (PSO), namely, IPOQEA [23], is designed. An IPOQEA-based gate allocation method is proposed to allocate the flights to suitable gates within different periods, which has better optimization ability in solving a gate allocation problem. For complex optimization problems, in the EMMSIQDE [24], a new differential mutation strategy of a difference vector is proposed to enhance the search ability and descent ability. Then, a new multipopulation mutation evolution mechanism is designed to ensure the relative independence of each subpopulation and the population diversity. A new optimal mutation strategy based on the complementary advantages of five mutation strategies is designed to develop a novel improved DE algorithm with the wavelet basis function, named WMSDE, which can improve the search quality, accelerate convergence, and avoid fall into local optimum and stagnation [25]. To avoid premature convergence and improve the global search ability, an improved quantum-inspired differential evolution (MSIQDE), namely, MSIQDE algorithm, based on making use of the merits of the Mexh wavelet function, standard normal distribution, adaptive quantum state update, and quantum nongate mutation is proposed [26].

The main aim of this paper is to propose an REII method based on the CNN by taking the advantages of EMD and bispectrum. First, preprocessing prepares the proper data sequence. Secondly, we combine the Hilbert–Huang Transform (HHT) spectrum and bispectrum to obtain the signal image. Then, we optimize the CNN algorithm. Finally, the simulation proves that our proposed method achieves outstanding performance for REII.

2. Emitter Individual Identification Method

In this section, we introduce the REII method based on the CNN. The method's block diagram is presented in Figure 1. The signal is preprocessed first, then in order to avoid loss of information and achieve the potential identification performance improvement, the transformed spectral data are directly input to the CNN, the CNN is optimized accordingly, and finally, the identification result is obtained.

2.1. Preprocessing. To avoid the influence of signal amplitude on identification, the received radar emitter signal data need to be normalized. For the original signal sequence $x(t)$, we find its maximum value $\max_{x(t)}$ and its minimum value $\min_{x(t)}$, and then, the normalization formula is as follows:

$$x_n(t) = \frac{x(t) - \max_{x(t)}}{\max_{x(t)} - \min_{x(t)}}. \quad (1)$$

2.2. HHT. The fundamental of HHT consists of the empirical mode decomposition (EMD) and Hilbert spectrum analysis. The former is a sifting process to decompose any signal into an infinite set of intrinsic mode function (IMF), while the latter offers the time-frequency distribution, referred to as the Hilbert spectrum, by performing the Hilbert transform on each IMF [22]. We propose an REII method based on the CNN, and the HHT spectrum and bispectrum are combined to form an image of the signal.

The core algorithm of HHT is EMD, and the goal of EMD is to obtain an Intrinsic Mode Function (IMF). The steps are as follows:

- (1) The upper and lower envelopes $b_{\max}(t)$ and $b_{\min}(t)$ are obtained by fitting the extreme points of the normalized sequence $x_n(t)$, and their average value is

$$a_1(t) = \frac{b_{\max}(t) + b_{\min}(t)}{2}. \quad (2)$$

- (2) $a_1(t)$ is subtracted from the data sequence:

$$p_1(t) = x_n(t) - a_1(t). \quad (3)$$

Whether $p_1(t)$ meets the requirements of the IMF is determined [8]. If so, it is regarded as the first IMF component; otherwise, we go to step 3.

- (3) With $p_1(t)$ as the new initial data, steps 1 and 2 are repeated until the requirements of IMF are met. After looping k times, the expression is as follows:

$$p_{1k}(t) = p_{1(k-1)}(t) - a_{1k}(t). \quad (4)$$

- (4) After the first screening, the first IMF obtained was separated:

$$d_1(t) = x_n(t) - \text{imf}_1(t). \quad (5)$$

Then, $d_1(t)$ is used as the new initial data, and steps 1 to 4 are performed in a loop. After looping n times, the expression is as follows:

$$d_n(t) = d_{n-1}(t) - \text{imf}_n(t). \quad (6)$$

- (5) HHT time-frequency spectrum can be obtained by performing Hilbert transform on each IMF. Assuming that $R_i(f, t)$ ($i = 1, 2, \dots, n$) is obtained after each IMF is transformed, the HHT spectrum expression is as follows:

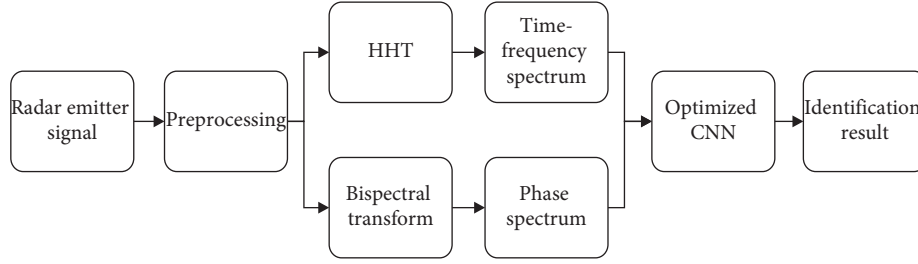


FIGURE 1: Block diagram of the proposed method.

$$\text{TF}(f, t) = \sum_{i=1}^n R_i(f, t). \quad (7)$$

$$\sum_{\tau_1=-\infty}^{\infty} \sum_{\tau_2=-\infty}^{\infty} |c_{3x}(\tau_1, \tau_2)| < \infty. \quad (13)$$

2.3. Bispectral Transform. In the higher-order spectrum, bispectrum has the lowest order, so it has the lowest complexity and strong practicability.

Let $f(x_1, x_2, \dots, x_k)$ be the joint probability density function of the continuous random variable x_1, x_2, \dots, x_k , and the first joint feature function is defined as

$$\begin{aligned} \Phi(w_1, w_2, \dots, w_k) &= E \left\{ e^{j(w_1 x_1 + w_2 x_2 + \dots + w_k x_k)} \right\}, \\ &= \int_{-\infty}^{+\infty} \dots \int_{-\infty}^{+\infty} f(x_1, x_2, \dots, x_k) \\ &\quad e^{j(w_1 x_1 + w_2 x_2 + \dots + w_k x_k)} dx_1 dx_2 \dots dx_k. \end{aligned} \quad (8)$$

The second joint feature function expression is

$$\Psi(w_1, w_2, \dots, w_k) = \ln \Phi(w_1, w_2, \dots, w_k). \quad (9)$$

Then, we can get the r -th joint cumulant of $x_1 \dots x_k$, $r = r_1 + r_2 + \dots + r_k$:

$$c_r = \text{cum}(x_1^{r_1} \dots x_k^{r_k}) = (-j)^r \frac{d^r \Psi(w_1, w_2, \dots, w_k)}{dw_1^{r_1} \dots dw_k^{r_k}} \Big|_{w_1=\dots=w_k=0}. \quad (10)$$

When $r_1 = r_2 = \dots = r_k = 1$, the k -th order cumulant expression of x_1, x_2, \dots, x_k is as follows:

$$c_k = \text{cum}(x_1 \dots x_k) = (-j)^k \frac{d^k \ln \Phi(w_1 \dots w_k)}{dw_1 \dots dw_k} \Big|_{w_1=\dots=w_k=0}. \quad (11)$$

For continuous rand signals $x(t)$, let $x_1 = x(t), \dots, x_k = x(t + \tau_{k-1})$. Then, the k -th order cumulant of $x(t)$ is expressed as

$$c_{kx}(\tau_1, \tau_2, \dots, \tau_{k-1}) = \text{cum}[x(t), x(t + \tau_1), x(t + \tau_2), \dots, x(t + \tau_{k-1})]. \quad (12)$$

We take $k=3$, if the following formula holds:

Then, the bispectrum expression is as follows:

$$B_x(\omega_1, \omega_2) = \sum_{\tau_1=-\infty}^{\infty} \sum_{\tau_2=-\infty}^{\infty} c_{3x}(\tau_1, \tau_2) e^{-j(\omega_1 \tau_1 + \omega_2 \tau_2)}. \quad (14)$$

2.4. CNN Optimization. REII is different from the traditional pattern recognition task. It has high requirements for identification accuracy and real-time performance, and the input is obviously different from ordinary image data. Therefore, for the purpose of enhancing the network's ability to extract signal fingerprint features, improve identification accuracy, and reduce identification time, it is necessary to optimize the general CNN to better meet the practical application needs.

2.4.1. Number of Convolutional Kernels. A type of convolutional kernel can extract a specific data pattern feature. In traditional pattern-recognition tasks, multiple convolutional kernels are used to fully extract different pattern features to improve accuracy. However, the composition of the signal spectrum is relatively simple, and the number of pattern features is relatively small. Using too many convolutional kernels will increase network redundancy, increase network scale, and bring negative effects. Therefore, the number of convolutional kernels needs to be optimized.

2.4.2. Convolutional Kernel Size and Convolutional Kernel Step Size. Small convolutional kernels have fewer parameters and lower computational complexity, but the signal spectrum features are often sparser than ordinary image features. It is difficult for small convolutional kernels to completely extract sparse pattern features. Convolutional kernel slides on data in certain step size. To avoid information loss, the step size is usually smaller than the convolutional kernel size. A smaller convolutional kernel step size can make the convolutional kernel scan the data more fully, but it may also cause repeated calculation and fitting of the noise distributed in the signal spectrum, which reduces

the generalization ability of the model and affects the identification accuracy. Therefore, the size and step size of the convolutional kernel need to be optimized.

2.4.3. Number of Convolutional Layers. The increase of depth is one of the important reasons why the performance of deep learning models is superior to that of shallow models. Generally, within a certain range, with the increase in the number of layers, the network's nonlinear expression ability is enhanced, the features it extracts are more distinguished, and the pattern recognition performance is better. However, the abstraction of signal spectrum data features is at a low level, which makes deep networks unnecessary. In addition, a deep network has high complexity and low training efficiency, which affects the speed of recognition and model update.

3. Experiment and Result Analysis

The measured signal data of three radar emitters are used in this paper, each radar emitter has 500 signals, and the modulation and working modes of the signals are the same. In order to simplify the optimization process, a fixed network layer connection structure is adopted, which in turn, includes a convolutional layer, a batch normalization (BN) layer [27], an activation layer, and a pooling layer. The introduction of the BN layer in the CNN can alleviate the problem of gradient disappearance, speed up the training speed, and reduce the manual parameter adjustment process. At the same time, in order to facilitate parameter selection, each layer of convolutional layers is set to contain the same number of convolutional kernels, and the last part of the network is a fully connected layer and a classification output layer. The size of the convolutional kernel is set to 3×3 , and the steps of the convolutional kernels are set to be 1 and 2, respectively. CNNs with different numbers of convolutional layers and each layer with different numbers of convolutional kernels are trained. The trained optimal model is used to identify the test set to achieve accuracy. The result is shown in Figure 2.

The results in Figure 2 address that consistent with the previous analysis, different parameter settings have a significant impact on identification performance. When the convolutional kernel step is 1, the model is easy to repeatedly calculate and fit the noise distributed in the input spectrum, which makes the generalization ability poor. Therefore, the overall identification accuracy is low, and it fluctuates with the number of convolutional kernels. When the convolutional kernel step is 2, it can avoid the influence of the noise to a certain extent and extract the signal fingerprint features more efficiently.

Then, the convolutional kernel size is set to be 5×5 , 7×7 , and training and testing are performed under different numbers of convolutional kernels and convolutional layers. The results are shown in Figures 3 and 4.

From the results mentioned above, we can draw the following conclusions:

- (1) When the convolutional kernel size, the convolutional kernel step size, and the number of convolutional layers are fixed, the identification accuracy increases with the number of convolutional kernels and gradually stabilizes. The increase in the number of convolutional kernels can make the network extract the signal fingerprint features more fully, and after the fingerprint features are fully extracted, continuing to increase the convolutional kernel will cause the network parameters to be redundant and the identification accuracy will not be further improved.
- (2) In general, the identification performance is better when the number of convolutional layers is 2 and the convolutional kernel step size is 2. On this basis, an increase in the number of convolutional layers will lead to a decrease in feature dimension; an increase in the convolutional kernel step size will lead to insufficient feature extraction, and both cases will lead to a decrease in identification performance.
- (3) When the number of convolutional layers is 2 and the convolutional kernel step size is 2, the identification accuracy is relatively stable while being at a high level, and the robustness to changes in the number of convolutional kernels is strong, indicating that the signal fingerprint feature extraction ability of the network is strong, and the extracted signal fingerprint feature dimension and abstraction level reaches a good balance.
- (4) When the number of convolutional layers is 2 and the convolutional kernel step size is 2, the identification performance of 5×5 and 7×7 convolutional kernel networks is similar, and both are better than 3×3 convolutional kernel networks. Among them, when the convolutional kernel size is 5×5 and the number of convolution kernels is 14, the identification accuracy is the highest, reaching 99.56%.

In summary, the optimized CNN parameters are set as follows: the convolutional kernel is 5×5 , convolution kernel step size is 2, number of convolutional layers is 2, and number of convolutional kernels per layer is 14.

4. Performance Evaluation

In this section, we evaluate the performance of the proposed method. The complexity determines the training and prediction time of the model. If the complexity is too high, it will lead to a lot of time for model training and prediction, neither to quickly verify ideas and improve the model, nor to achieve rapid prediction. The number of iterations trained in the CNN model determines the time complexity of the algorithm. Therefore, this section gives the curve of the loss, and accuracy of the optimal

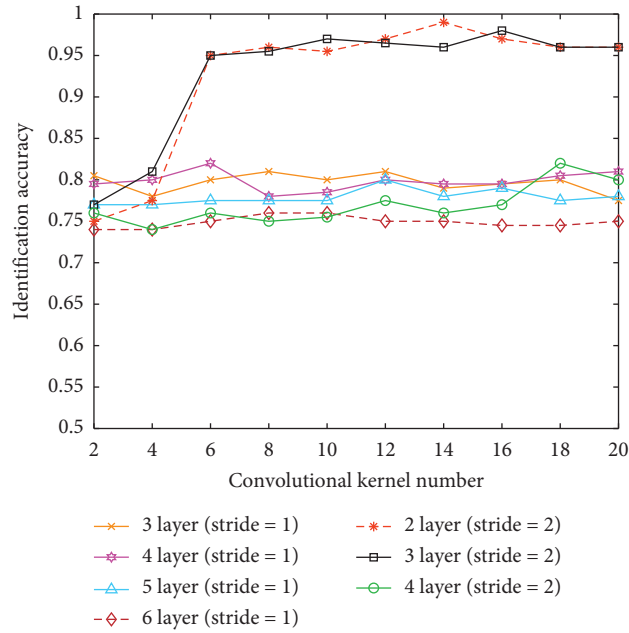


FIGURE 2: 3x3 convolutional kernel identification accuracy.

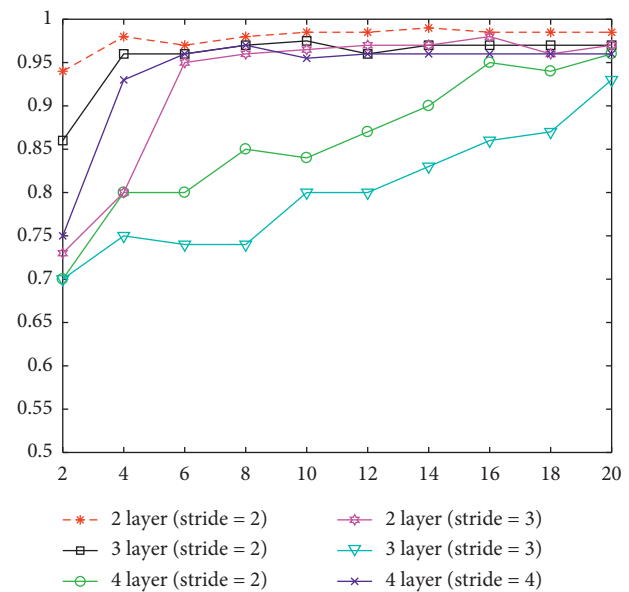


FIGURE 3: 5x5 convolutional kernel identification accuracy curve.

parameter CNN with the number of training iterations on the test dataset is shown in Figure 5. The relationship between complexity and model performance is reflected. It can be seen that as the number of iterations increases, the network loss decreases and gradually converges; the accuracy gradually rises and stabilizes at a high level. This shows that, after sufficient training, the CNN has learned effective signal fingerprint pattern features and can distinguish different radar emitter individuals effectively.

The signal preprocessing, HHT transform, and bispectral transform are comprehensively designed as a preprocessing

and transformation module (module 1), and the trained CNN model is designed as an identification module (module 2). The two modules are connected in series to form an identification system. The performance evaluation results of the system are shown in Table 1.

Table 1 shows that the identification accuracy of radar emitter individuals by the optimized CNN is as high as 99.56%. In terms of recognition speed, the computational complexity of module 1 is relatively high and it takes a relatively long time, while the computational complexity of module 2 is relatively low and it takes less time. The system

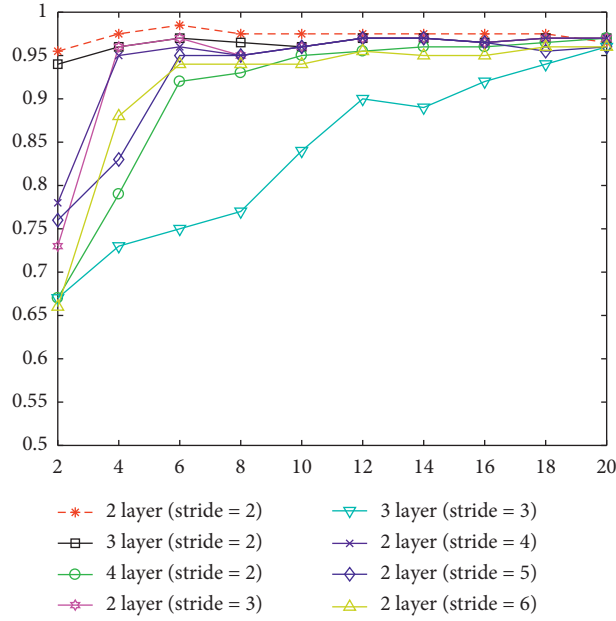
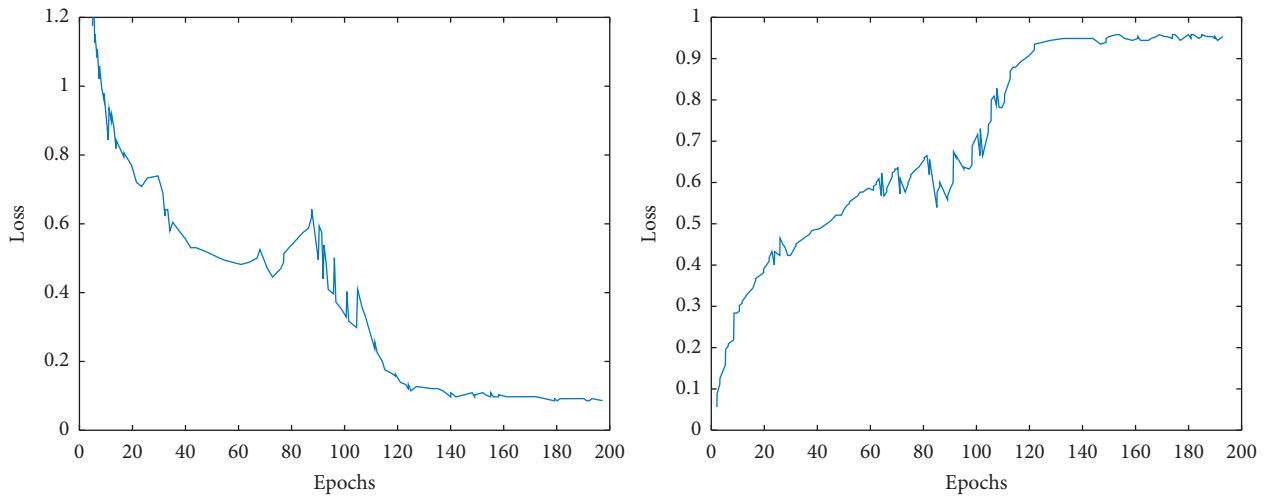
FIGURE 4: 7×7 convolutional kernel identification accuracy curve.

FIGURE 5: Loss and accuracy curve.

TABLE 1: System performance evaluation results.

Signal number	450
Correct number	448
Identification accuracy	99.56%
Time consumed by module 1	46.32 s
Time consumed by module 2	0.30 s
Total time	46.62 s
Average time	0.104 s

takes only about 0.104 s to identify each signal, which can meet the needs of practical applications.

We simulate the radars to send and receive the signal with Python. Meanwhile, we collect real data from several WLAN devices to optimize the simulation parameters.

In this simulation environment, we will control the power of each device to send or receive the signal. The

distance is fixed to ensure the results can be compared with each other.

We also compete with the simulation program with several hundred signals. After collecting the data from the WLAN devices, we will adjust the signals' parameters.

With the Monte Carlo method, the signals will be recorded, and only the average value will be input into the final CNN network.

The simulation platform is Tensorflow with Intel i7-8700 four cores CPU, 512 GB memory, and GeForce GTX 1080 Ti Graphics Cards.

In order to further verify the effectiveness of the proposed method, we compare it to other typical identification methods, including the traditional SIB method, the method proposed in [14, 15], and [21]. The results are shown in Table 2.

TABLE 2: Comparison of different identification methods.

Method	SIB (%)	Reference [10] (%)	Reference [11] (%)	Reference [16] (%)	This paper (%)
Accuracy	81.33	83.11	84	81.27	99.56

In Table 2, compared to the SIB method and the methods in the references, the CNN-based identification method proposed in this paper achieves a performance improvement of more than 10%. In addition, the proposed identification method has low computational complexity, strong generalization ability, and adaptability and reduces the difficulty and uncertainty of feature engineering, which validates the effectiveness of deep-learning applications in REII.

5. Conclusions

In this paper, we propose an REII method based on the CNN. Through the analysis of HHT and bispectral theory, combined with the advantages of deep-learning techniques, a CNN-based REII method with stronger generalization ability and adaptability is successfully implemented. The HHT spectrum and bispectrum are combined, and the signal image obtained is identified by the optimized CNN to form an image of the signal. The comparative experimental results based on the measured signal data and other typical identification methods show that the identification accuracy of the proposed method is higher than 99%, and the computational complexity is low, which can meet the requirements of practical applications.

Data Availability

The data can be requested via e-mail 15601001217@163.com.

Conflicts of Interest

The authors declare that there are no conflicts of interest regarding the publication of this paper.

Acknowledgments

This work was supported in part by the National Natural Science Foundation of China under Grant no. 61471066.

References

- [1] R. Guan, "New network planning technology based on 5G ultra-dense networking," *Communication World*, vol. 27, no. 06, p. 57, 2020.
- [2] F. Mekuria and L. Mfupe, "Spectrum sharing for unlicensed 5G networks," in *Proceedings of the 2019 IEEE Wireless Communications and Networking Conference (WCNC)*, pp. 1–5, Marrakesh, Morocco, April 2019.
- [3] X. Sun, "5G mobile communication development trend and key technology analysis," *Metallurgical Management*, vol. 13, pp. 138–139, 2020.
- [4] X. Wang, G. Huang, C. Ma, W. Tian, and J. Gao, "Convolutional neural network applied to specific emitter identification based on pulse waveform images," *IET Radar, Sonar & Navigation*, vol. 14, no. 5, pp. 728–735, 2020.
- [5] K. Sa, D. Lang, C. Wang, and Y. Bai, "Specific emitter identification techniques for the internet of things," *IEEE Access*, vol. 8, pp. 1644–1652, 2020.
- [6] J. Allen, "Short term spectral analysis, synthesis, and modification by discrete Fourier transform," *IEEE Transactions on Acoustics, Speech, and Signal Processing*, vol. 25, no. 3, pp. 235–238, 1977.
- [7] W. Ye and Z. Yu, "Signal recognition method based on joint time-frequency radiation source," *Electronic Information Countermeasure Technology*, vol. 33, no. 5, pp. 18–21, 2018.
- [8] E. P. Wigner, "On the quantum correction for thermodynamic equilibrium," *Physical Review*, vol. 40, no. 40, pp. 749–759, 1932.
- [9] R. G. Stockwell, L. Mansinha, and R. P. Lowe, "Localization of the complex spectrum: the S transform," *IEEE Transactions on Signal Processing*, vol. 44, no. 4, pp. 998–1001, 2002.
- [10] J. Morlet, G. Arens, E. Fourgeau et al., "Wave propagation and sampling theory—part I: complex signal and scattering in multilayered media," *Geophysics*, vol. 47, no. 2, p. 203, 2013.
- [11] N. E. Huang, Z. Shen, S. R. Long et al., "The empirical mode decomposition and the Hilbert spectrum for nonlinear and non-stationary time series analysis," *Proceedings of the Royal Society of London. Series A: Mathematical, Physical and Engineering Sciences*, vol. 454, no. 1971, pp. 903–995, 1998.
- [12] T. Thayaparan, L. Stankovic, M. Amin, V. Chen, L. Cohen, and B. Boashash, "Editorial: time-frequency approach to radar detection, imaging, and classification," *IET Signal Processing*, vol. 4, no. 3, pp. 197–200, 2010.
- [13] F. Lin, S. Sun, X. Hou, and Y. Liu, "Radar fingerprint feature extraction based on VMD," in *Proceedings of the 2019 19th International Symposium on Communications and Information Technologies (ISCIT)*, pp. 426–429, Ho Chi Minh City, Vietnam, September 2019.
- [14] S. Xu et al., "Communication emitter individual identification based on SIB/PCA," *Journal of Huazhong University of Science and Technology: Natural Science Edition*, vol. 7, pp. 14–17, 2008.
- [15] M. Liu et al., "Radio fingerprint identification based on rectangular integral bispectrum and kernel principal component analysis," *Journal of Northwest University (Natural Science Edition)*, vol. 41, no. 1, pp. 43–47, 2011.
- [16] V. Chandran and S. L. Elgar, "Pattern recognition using invariants defined from higher order spectra- one dimensional inputs," *IEEE Transactions on Signal Processing*, vol. 41, no. 1, p. 205, 1993.
- [17] J. K. Tugnait, "Detection of non-Gaussian signals using integrated polyspectrum," *IEEE Transactions on Signal Processing*, vol. 42, no. 11, pp. 3137–3149, 1993.
- [18] X. Liao and Z. Bao, "Circularly integrated bispectra: novel shift invariant features for high-resolution radar target recognition," *Electronics Letters*, vol. 34, no. 19, p. 1879, 1998.
- [19] J. Ma et al., "Spatial target recognition algorithm based on local integral bispectrum," *Systems Engineering and Electronics*, vol. 8, pp. 1490–1493, 2005.
- [20] N. X. Kang, M. H. He, J. Han et al., "Radar emitter fingerprint recognition based on bispectrum and SURF feature," in *Proceedings of the 2016 CIE International Conference on Radar (RADAR)*, IEEE, Guangzhou, China, October 2016.

- [21] N. Li et al., "Radar emitter identification based on bispectrum," *Journal of Beijing Union University*, vol. 26, no. 2, pp. 26–33, 2012.
- [22] J. Zhang, F. Wang, O. A. Dobre, and Z. Zhong, "Specific emitter identification via hilbert-huang transform in single-hop and relaying scenarios," *IEEE Transactions on Information Forensics and Security*, vol. 11, no. 6, pp. 1192–1205, 2016.
- [23] W. Deng, J. Xu, H. Zhao, and Y. Song, "A novel gate resource allocation method using improved PSO-based QEA," *IEEE Transactions on Intelligent Transportation Systems*, pp. 1–9, 2020.
- [24] W. Deng, J. Xu, X.-Z. Gao, and H. Zhao, "An enhanced MSIQDE algorithm with novel multiple strategies for global optimization problems," *IEEE Transactions on Systems, Man, and Cybernetics: Systems*, pp. 1–9, 2020.
- [25] Wu Deng, J. Xu, Y. Song et al., "Differential evolution algorithm with wavelet basis function and optimal mutation strategy for complex optimization problem," *Applied Soft Computing*, vol. 100, Article ID 106724, 2021.
- [26] W. Deng, H. Liu, J. Xu, H. Zhao, and Y. Song, "An improved quantum-inspired differential evolution algorithm for deep belief network," *IEEE Transactions on Instrumentation and Measurement*, vol. 69, no. 10, pp. 7319–7327, 2020.
- [27] S. Ioffe and C. Szegedy, "Batch normalization: accelerating deep network training by reducing internal covariate shift," in *Proceedings of the International Conference on International Conference on Machine Learning*, JMLR.org, Lille, France, July 2015.